The EMBO Journal vol.15 no.4 pp.695–704, 1996

Phragmoplastin, a dynamin-like protein associated with cell plate formation in plants

Xiangju Gu and Desh Pal S.Verma[1]

Department of Molecular Genetics, Ohio State Biochemistry Program and Plant Biotechnology Center, The Ohio State University, 1060 Carmack Road, Columbus, OH 43210, USA

[1]Corresponding author

Cytokinesis in a plant cell is accomplished by the formation of a cell plate in the center of the phragmoplast. Little is known of the molecular events associated with this process. In this study, we report the identification of a dynamin-like protein from soybean and demonstrate that this protein is associated with the formation of the cell plate. Plant dynamin-like (PDL) protein contains 610 amino acids showing high homology with other members of the dynamin protein family. Western blot experiments demonstrated that it is associated with the non-ionic detergent-resistant fraction of membranes. Indirect immunofluorescence microscopy localized PDL to the cell plate in dividing soybean root tip cells. Double labeling experiments demonstrated that, unlike phragmoplast microtubules which are concentrated on the periphery of the forming plate, PDL is located across the whole width of the newly formed cell plate. Based on the temporal and spatial organization of PDL in the phragmoplast, we termed this protein 'phragmoplastin'. The data suggest that phragmoplastin may be associated with exocytic vesicles that are depositing cell plate material during cytokinesis in the plant cell.

Keywords: cell plate/cytokinesis/dynamin/exocytosis/immunofluorescence

Introduction

Dynamin is one of the members of a group of newly identified high molecular weight proteins with GTPase activity (Obar *et al.*, 1990). Several yeast and animal proteins including VPS1 and Mxs have been grouped into the dynamin family based on the high homology in their GTP binding regions. Animal dynamins have been shown to be involved in endocytosis (Shpetner and Vallee, 1989; Vallee and Okamoto, 1995). VPS1 of yeast is involved in vacuolar protein sorting and trans-Golgi protein retention (Rothman *et al.*, 1990; Vater *et al.*, 1992; Wilsbach and Payne, 1993). Mxs are interferon-induced proteins of vertebrate cells which have anti-virus function (Nakayama *et al.*, 1991; Staeheli *et al.*, 1993).

Experiments with both transfected culture cells and the *Drosophila* mutant *shibire* demonstrated that dynamin is required for the budding of the endocytic vesicles from the plasma membrane (Poodry *et al.*, 1973; Chen *et al.*, 1991; van de Bliek and Meyerowitz, 1991; Herskovits *et al.*, 1993a; van de Bliek *et al.*, 1993). Mutation in the dynamin gene had no effect on the formation and invagination of the coated pits, but the pinching off of the vesicles is specifically inhibited, leading to the accumulation of elongated membrane tubules on the plasma membrane. Recently, it has been shown that dynamin can self-assemble into rings and stacks of interconnected rings in the test tube, and these ring-like structures enable dynamin to wrap around the neck of the endocytic vesicles and help them bud off from the plasma membrane (Hinshaw and Schmid, 1995; Takei *et al.*, 1995). In addition to dynamin, Mx proteins can also polymerize into horseshoe-like structures *in vitro*, and these C-shaped structures can transform into tightly packed helical structures with similar parameters to those of dynamin (Nakayama *et al.*, 1993). It is suggested that Mx proteins interfere with virus infection by wrapping around some as yet unidentified structures in the nuclei (Nakayama *et al.*, 1993). Another dynamin-like protein, VPS1 of yeast, which is involved in protein sorting, also has the self-assembly motif of Mx. It is suggested that VPS1 might use the same mechanism to facilitate membrane protrusion in the Golgi apparatus (Kelly, 1995). Thus, it appears that the ability to form helical structures around tubular templates might be the hidden link between proteins of the dynamin family.

During cell division in plants, a cell plate is formed (Hepler, 1982; Baskin and Cande, 1990), making cytokinesis in the plant cell different from that in animal and yeast cells (Fishkind and Wang, 1995). The cell plate is a disc-like membrane-bounded structure formed by fusion of Golgi-derived vesicles. These vesicles deposit the cell wall material forming the cell plate that partitions the two daughter cells (Baskin and Cande, 1990). Although a large amount of information has been accumulated about the process of cell plate formation in plants, most of this is based on light and electron microscopic observations and the effect of various inhibitors on the cell plate formation (Gunning and Wick, 1985; Hepler and Bonsigore, 1990; Wolniak and Larsen, 1995). In plants, the plane of cell division is predetermined before the onset of mitosis. The first indication of the future cell division plane is the appearance of the pre-prophase band (PPB), an annular cortical microtubule array which lies just beneath the plasma membrane. Even though the PPB disappears during mitosis, the division plane is somehow 'imprinted' and the future cell plate fuses with the parental membrane precisely at this site (Gunning and Wick, 1985). The formation of the cell plate actually begins at late anaphase and involves a coordinated delivery, aggregation and fusion of Golgi-derived vesicles. The final step of the new cell formation requires the fusion of the margins of the new cell plate with the predetermined fusion site in the parental plasma membrane (Hepler, 1982).

Cell plate formation is not only important for separating the two daughter cells *per se*, it is also an important event

which determines plant morphogenesis. Encased in rigid cell walls, plant cells do not migrate after cell division as animal cells do. Therefore, plant morphogenesis depends on orderly cell division and controlled cell elongation. The precisely patterned geometrical relationship established during cytokinesis is usually retained despite cell enlargement, and has great impact on the direction of cell elongation. Thus, the division plane is crucial to plant tissue morphology. Despite its importance, little is known about the mechanisms that control cell plate formation at the molecular level. We report here the identification of a dynamin-like protein from soybean and demonstrate that this protein is associated with cell plate formation in plants.

Results

Isolation of soybean cDNAs encoding dynamin-like protein

In an effort to understand endocytic and exocytic processes in plant cells, we attempted to isolate homologs of dynamin. Two soybean cDNA clones encoding dynamin-like proteins were isolated by PCR using synthetic oligonucleotide primers based on the conserved motifs in the animal dynamins and yeast VPS1. A single 500 bp fragment was obtained after RT-PCR. Sequencing of this fragment showed significant DNA homology to animal dynamins. This fragment was used as a probe to screen a soybean nodule λ-Zap II cDNA library. Four positive clones were identified after screening 1×10^6 plaques. Sequence analysis indicated that three of these clones, including the longest one pPDL5, are encoded by the same gene. The other clone, pPDL12, is encoded by a different gene. Both pPDL5 and pPDL12 appear to contain nearly full-length cDNA inserts with poly(A) tails and with 126 bp (pPDL5) and 159 bp (pPDL12) 5′-non-coding regions. Each of these two sequences contains a long open reading frame of 1830 bp corresponding to a putative protein of 610 amino acids in length with a calculated mol. wt of 68.3 kDa (Figure 1A). The two clones differ in the N-terminal and C-terminal non-coding regions, but share very high homology in their coding regions. There are only nine amino acid differences between the two proteins scattered all along the length of the sequence.

A search of the Genbank protein database revealed that plant dynamin-like protein (PDL) shared high homology with other dynamin family proteins. Animal dynamins showed the highest homology, followed by VPS1 of yeast and Mxs of vertebrates. The homology is especially high in the GTP binding domain located in the N-terminal region of these proteins, with 58% identical residues in the first 300 amino acids between PDL and dynamin. Similarly to VPS1 and Mx, PDL lacked the very C-terminal proline-rich domain of dynamin which was involved in microtubule and SH3 domain binding and phosphorylation by protein kinase C (Robinson *et al.*, 1993). However, there is a putative calcium/calmodulin-dependent protein kinase and cAMP-dependent protein kinase A site in the C-terminus (position 574) of PDL. The overall identity between PDL and rat brain dynamin was found to be 41.6%, whereas the identity between PDL and VPS1 was only 38.1%.

Like dynamin and other G-proteins, PDL has three consensus sequences involved in GTP binding (Bourne *et al.*, 1991). The G1 region $G(X)_4GK(ST)$ (position 41–48), the G3 region DX_2G (position 142–145) and the G4 region (TN)(KQ)XD (position 211–214) were perfectly conserved in PDL, suggesting that it is also a GTP binding protein (see below). In addition, PDL shared high homology in the self-assembly motif, especially in region 1, with Mx1 (Figure 1B). These regions were highly conserved among other members of this protein family. In fact, the so-called dynamin signature sequence is present in region 1 of the self-assembly motifs (Nakayama *et al.*, 1993). Since both Mx and dynamin have been shown to be able to self-assemble into polymers, it is very likely that PDL has the ability to form polymers on its own. Despite this extensive homology of PDL with the dynamin family, the rat dynamin antibody R2 (Herskovits *et al.*, 1993a) did not cross-react with PDL, and PDL was unable to complement the yeast *vps1* mutant (data not shown; Robinson *et al.*, 1988).

PDL is a GTPase

In order to obtain purified PDL protein for GTPase assay and for antibody preparation, the insert from pPDL12 was subcloned into a bacterial expression vector pRSETC and the protein was expressed in *Escherichia coli*. Two constructs were made: the first contained the entire coding sequence of pPDL12 and the second construct was a truncated form of PDL. The internal *Hinc*II fragment of pPDL12 was removed to give a truncated protein which only contains the C-terminal 353 amino acids, whereas the whole GTP binding region in the N-terminus of the protein was removed. Both expressed proteins also contain a 35 amino acid polyhistidine metal binding domain and a four amino acid linker sequence in their N-termini. As shown in Figure 2, a protein band with a mol. wt of 72 kDa was induced after adding IPTG. This protein was able to bind to a Ni column and was purified by Ni affinity chromatography.

In comparison with other regulatory GTPases, dynamin proteins have high intrinsic GTP hydrolysis rates. Based on the extremely high sequence homology of PDL with other dynamin family proteins in the GTP binding domain, it was suggested that PDL might also hydrolyze GTP. To test this possibility, both the full-length and the truncated forms of PDL proteins were purified under native conditions, and a single band of protein was obtained after Ni chromatography. Figure 3A shows the protein blot of the *E.coli*-expressed PDL proteins. Their corresponding GTPase activities are shown in Figure 3B. Full-length PDL was able to hydrolyze GTP, whereas the truncated form did not. Similar fractions from the *E.coli* harboring the pRSETC vector (control) also did not hydrolyze GTP. This result demonstrated that, like dynamin and other members of the dynamin family, PDL protein could hydrolyze GTP without the requirement for other protein factors and thus had intrinsic GTPase activity.

The PDL gene is highly expressed in young tissues

We determined the expression levels of PDL in plant cells during plant development by Northern blot analysis. Total RNA from various tissues was isolated and hybridized with an *Eco*RI–*Xho*I fragment of pPDL12. As shown in Figure 4, the PDL gene was expressed in both root and nodule tissues. Root tips showed higher expression than

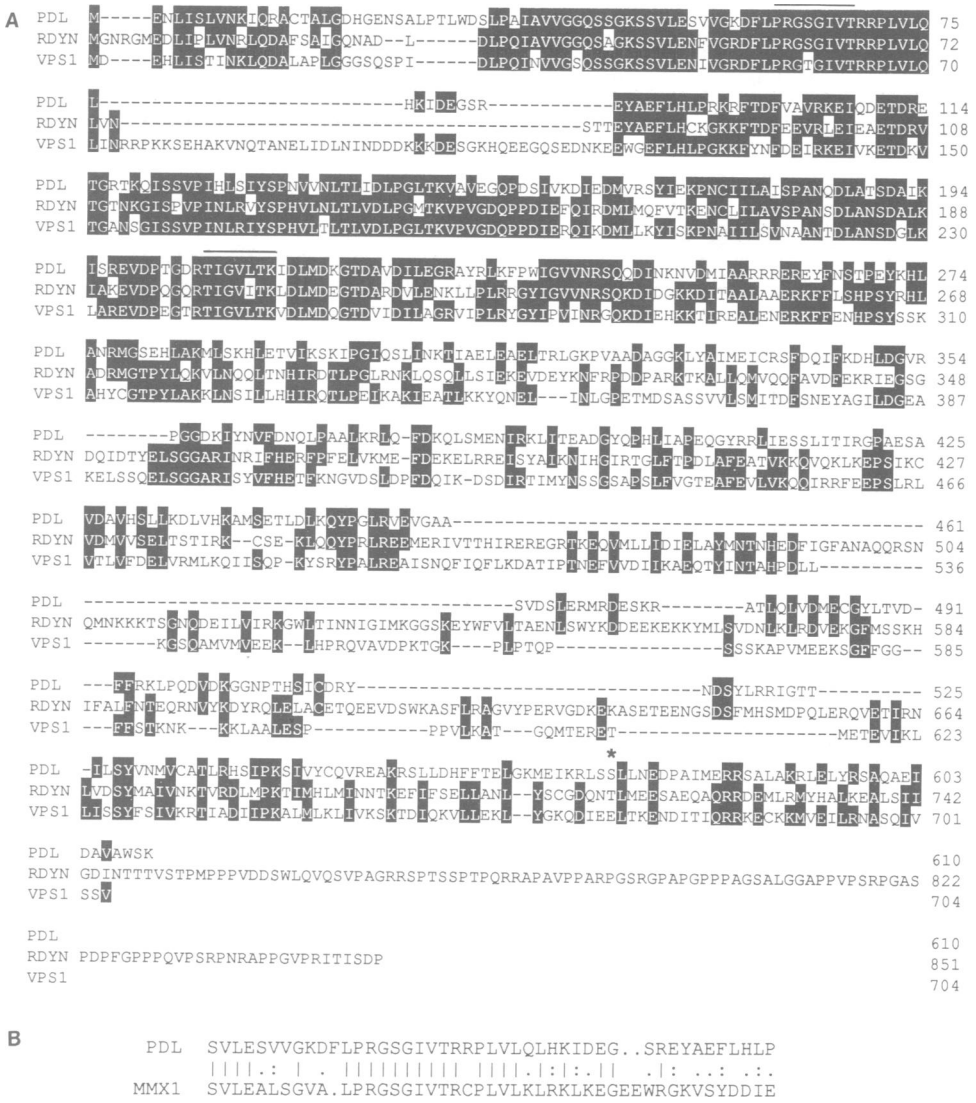

Fig. 1. Sequence analysis of plant dynamin-like (PDL) protein. (**A**) Sequence comparison of PDL, rat dynamin 1 (RDYN) and VPS1 of yeast. The sequences used for designing the PCR primers are indicated by horizontal lines. The putative phosphorylation site of PDL is indicated by an asterisk. (**B**) Comparison of the amino acid sequence of the putative self-assembly motif of PDL with that of Mx1. The upper line contains residues 49–93 of PDL, the lower line shows residues 51–96 of mouse Mx1. The solid vertical lines indicate identical amino acids, the dotted vertical lines indicate amino acids with similar properties.

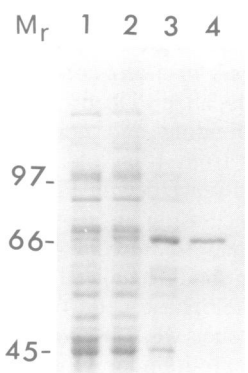

Fig. 2. Purification of *E.coli*-expressed PDL protein. Total extract from *E.coli* containing pEPDL-12 grown in LB medium before induction (lane 1) or after 3 h of induction with IPTG (lane 2) were separated on SDS–PAGE. The expressed protein was found mostly in the inclusion body fraction (lane 3) and was purified by Ni column chromatography under denaturing conditions (lane 4).

tissue from the elongation zone. PDL was also highly expressed in young nodules and, as the root nodules matured, the expression of PDL decreased. PDL expression was also higher in young leaves than in older leaves (data not shown). Thus, it appeared that the PDL gene was expressed in all tissues but its expression level was enhanced in young tissues having meristematic activity.

PDL protein is associated with the membrane fraction in plant cells

Western blotting was used to study the subcellular distribution of PDL. The post-mitochondrial supernatant of soybean root was centrifuged at 100 000 *g* to generate a crude microsomal fraction (P100) and a soluble fraction. The proteins were then analyzed by Western blot using polyclonal antibodies raised against the purified PDL. As shown in Figure 5, the antibody reacted strongly with a 68 kDa polypeptide band, which is in good agreement with the predicted mol. wt of 68.3 kDa for the PDL protein. This protein was mostly detected in the micro-

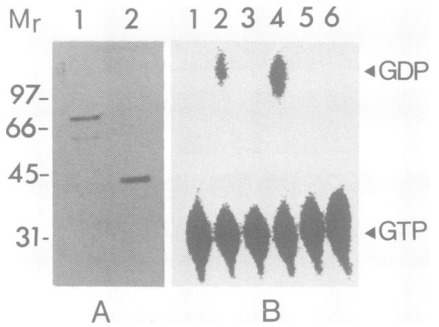

Fig. 3. GTPase activity of the *E.coli*-expressed PDL protein. (**A**) Protein blot showing *E.coli*-expressed PDL proteins. Lane 1, full-length PDL; lane 2, truncated PDL. (**B**) GTPase activities of purified PDL proteins (0.1 μg) from *E.coli* containing pEPDL-12 (lanes 2 and 4), pEPDL-12ΔHc (lanes 3 and 5) or the corresponding fraction from *E.coli* containing pRSETC (lane 6). Proteins were added to the reaction mixtures containing 130 μM (lanes 1, 2 and 3) or 13 μM (lanes 4, 5 and 6) cold GTP and 13 nM [α-^{32}P]GTP. The reactions were carried out as described in Materials and methods. Lane 1 is the negative control where no protein was added to the reaction mixture. The positions of GTP and GDP were identified using unlabeled reference nucleotides.

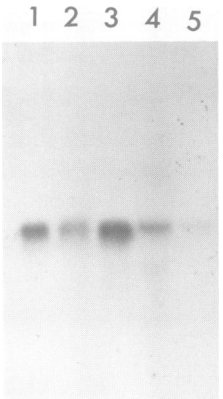

Fig. 4. Expression of PDL mRNA in different plant tissues. Total RNAs extracted from 4-day-old soybean root tips (lane 1), 4-day-old root elongation zone (lane 2); and 13-day-old (lane 3), 21-day-old (lane 4) and 30-day-old (lane 5) soybean root nodules were hybridized with the labeled *Eco*RI–*Xho*I insert of pPDL12. Hybridization was performed at 68°C. Equal amounts of total RNAs (30 μg) were loaded in each lane.

somal fraction. Only a very faint band was detected in the cytosol (Figure 5A). Similar results were obtained with root nodules and leaf tissues, suggesting a particulate localization of PDL in all plant tissues.

To test if PDL in the P100 pellet was associated with the microsomal membranes, this fraction was extracted with 0.1 M sodium carbonate (pH 11) and 0.5 M NaI, respectively. These treatments have been used to distinguish between the peripheral membrane proteins and the integral membrane proteins (Fujiki *et al.*, 1982). Even though these treatments solubilized ~50% of the total microsomal proteins, as judged from the SDS gel in our experiments (data not shown), neither sodium carbonate nor NaI could release PDL from the particulate/membrane fraction (Figure 5B).

We then attempted to solubilize PDL using different detergents. Triton X-100 (1%), deoxycholic acid (DOC, 1%) and SDS (1%) were tested. The particulate fraction

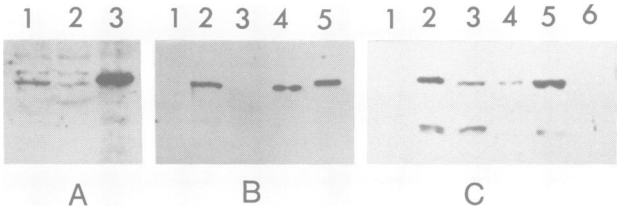

Fig. 5. Western blot analysis of PDL protein. (**A**) Subcellular distribution of PDL in soybean root cells. Total extract (lane 1), S100 (lane 2) and P100 (lane 3) of soybean root were separated on 10% SDS–PAGE and reacted with the anti-PDL polyclonal antibody. Equal amounts of proteins (50 μg) were loaded in each lane. (**B**) Solubility of particulate PDL-containing fraction in 0.1 M Na_2CO_3 (pH 11) and 0.5 M NaI. Lane 1, Na_2CO_3-soluble fraction; lane 2, Na_2CO_3-insoluble fraction; lane 3, NaI-soluble fraction; lane 4, NaI-insoluble fraction; lane 5, 72 kDa *E.coli*-expressed PDL protein. (**C**) Solubility of the particulate PDL-containing fraction in 1% Triton X-100, 1% DOC and 1% SDS. Lane 1, Triton X-100-soluble fraction; lane 2, Triton X-100-insoluble fraction; lane 3, DOC-soluble fraction; lane 4, DOC-insoluble fraction; lane 5, SDS-soluble fraction; lane 6, SDS-insoluble fraction.

was extracted with the detergents on ice for 30 min, and then centrifuged at 100 000 *g* for 30 min. Proteins in both the soluble fraction and the pellet were then analyzed by Western blot assay. As shown in Figure 5C, almost all of the PDL remained in the particulate fraction after treatment with 1% Triton X-100, and only a portion of the PDL protein could be solubilized by 1% DOC. This insolubility of PDL in non-ionic detergents was not due to oxidation and the formation of intermolecular disulfide bonds since 1% SDS released all of the PDL into solution. Similar observations for Mx protein have also been reported. About two-thirds of Mx in the mouse nuclear extract was insoluble at high concentrations of salt and a combination of salt and urea (Melen *et al.*, 1992; Nakayama *et al.*, 1993). In our experiments, 8 M urea could not solubilize PDL protein. PDL has no transmembrane domain and is a hydrophilic, charged protein. These results, together with the fact that PDL protein has the self-assembly motif, strongly suggested that, like Mx and dynamin, PDL also self-polymerizes in plant cells. It might be possible to prove this experimentally by expressing different length proteins of PDL in *E.coli*, as has been done with Mx1.

Association of PDL with cell plate formation during cytokinesis in plant cells

We attempted to localize PDL protein at the light microscopy level in dividing and non-dividing intact plant cells. Whole cells from 4-day-old soybean root tips were permeabilized and reacted with PDL antibodies. Indirect immunofluorescence using the affinity-purified PDL polyclonal antibody and fluorescein isothiocyanate (FITC)-labeled second antibody localized PDL to the region of cell plate in the telophase cells (Figure 6B and C). No cell plate fluorescence was observed in the control group of cells where the pre-immune serum was used as the first antibody (Figure 6E). The fluorescence of the cell plate occurred at a very early stage of cell plate formation and appeared to last until the cell plate reached the parental cell wall. After the new plasma membranes were formed in the respective daughter cells, the intense PDL staining of the cell plate disappeared (Figure 6D). Cells judged to be in other stages of cell division on the basis of 4′,6′-

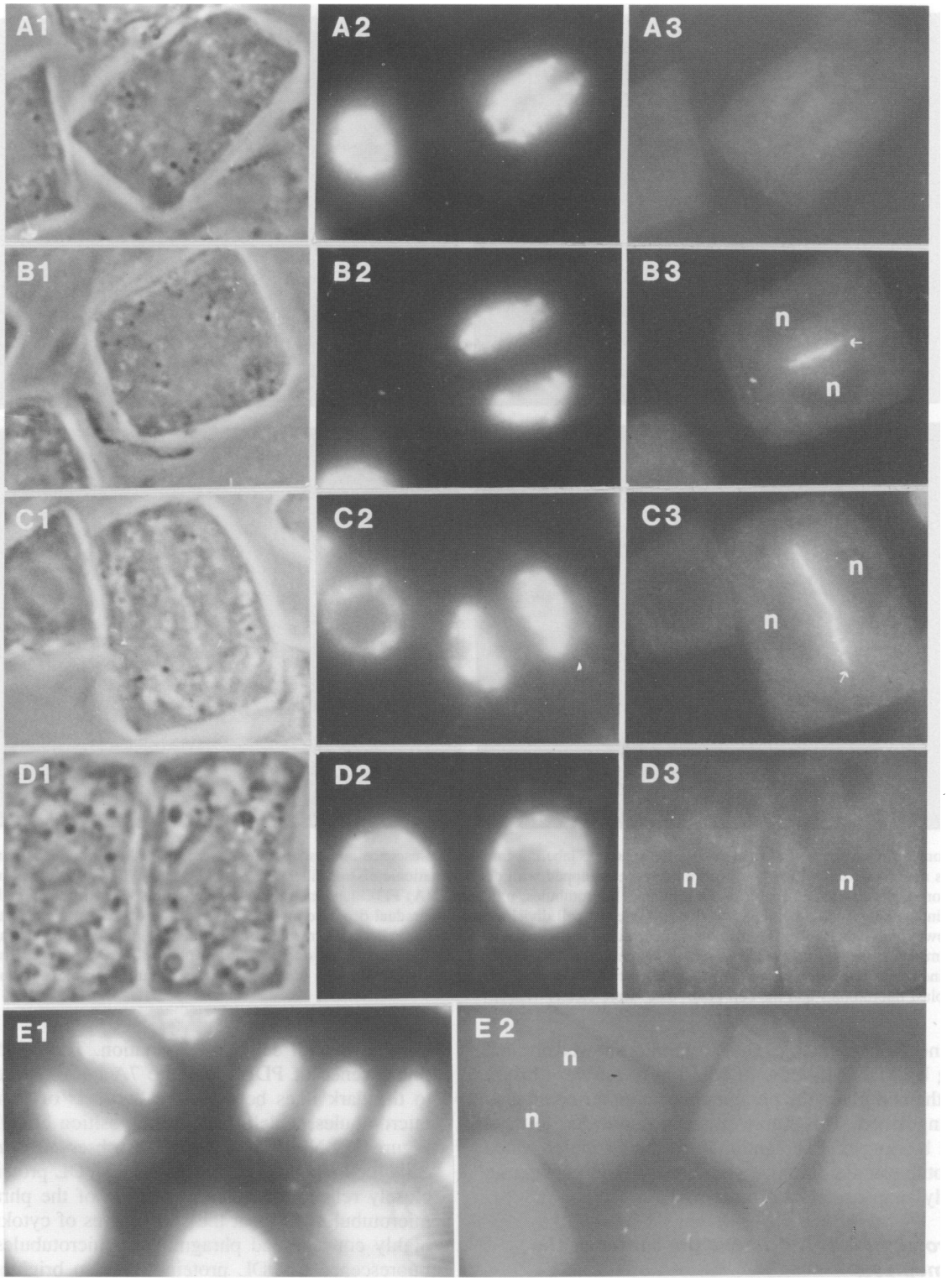

Fig. 6. Indirect immunofluorescence localization of PDL protein. In (A–D), the left-hand pictures show the phase contrast images, the right-hand pictures show the PDL immunofluorescence labeling and the middle images show the corresponding DAPI labeling. (E) is the control group of cells: the left-hand image shows the DAPI staining; the picture on the right is the immunofluorescence image using pre-immune serum as the first antibody. The arrow marks the position of the cell plate; n, nucleus. (**A**) Two sets of chromosome just begin to separate. At this stage, no cell plate could be distinguished by PDL antibody labeling or phase contrast microscopy. (**B**) At late anaphase or early telophase, the inter-zone region could be visualized with PDL antibody. Note that no cell plate was observed by phase contrast microscopy at this stage. (**C**) Telophase cell showing the late stage of cell plate formation. The PDL antibody reacted with the entire width of the cell plate. At this stage, the cell plate could be distinguished in the phase contrast image. (**D**) The two daughter cells have separated completely. No PDL fluorescence was observed on the newly formed cell plasma membranes and cell wall. At this stage, the PDL antibody gave a perinuclear particulate staining pattern. (**E**) Three cells in this control group were at telophase, but no reaction of pre-immune serum with cell plate was observed.

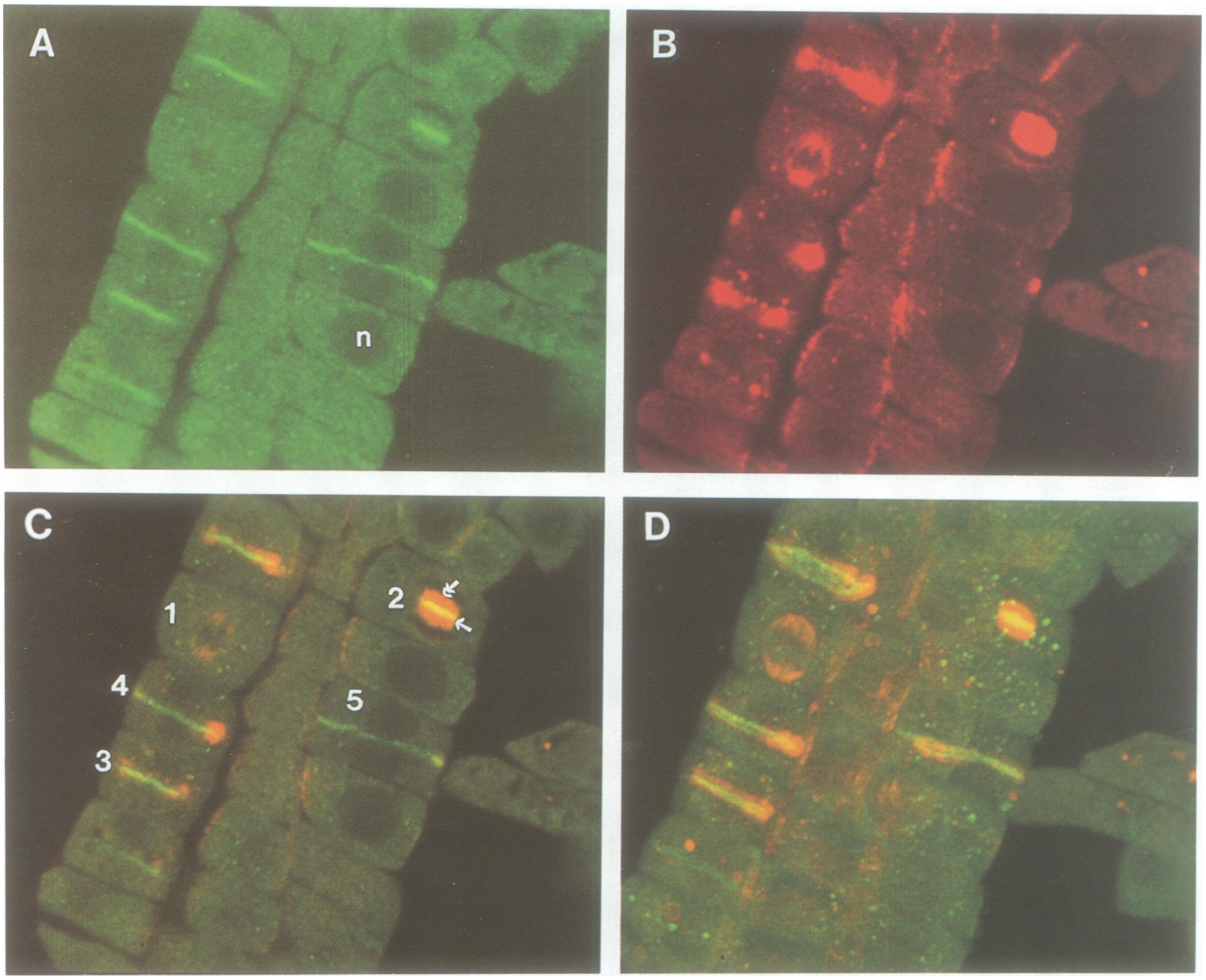

Fig. 7. Confocal visualization of phragmoplasts by double labeling immunofluorescence microscopy. Cells were reacted with both PDL and tubulin antibodies and visualized with a confocal microscope equipped with dual excitation/emission filter sets for FITC and TRITC. A single arrow marks the position of the cell plate; double arrows indicate microtubules; n, nucleus. (**A**) FITC labeling of PDL in dividing soybean root tip cells. Note the different intensities of PDL staining at different stages of cell division and the gradual decrease of PDL in the center of the phragmoplasts as cell plates grow outwards. (**B**) TRITC labeling of microtubules showing the mitotic spindle in the metaphase cell (cell #1) and the typical structures of the phragmoplasts during different stages of cytokinesis (cell #2, 3, 4 and 5). (**C**) Dual excitation/emission for both FITC and TRITC. The yellow colored line marks the region where PDL and microtubules overlap. (**D**) Projected 3-D images of phragmoplasts. Double ring-like structure of phragmoplast microtubles and the cell plate 'disc' were clearly visible.

diamidino-2-phenylindole (DAPI) staining showed no such staining by PDL antibody. In addition to the very bright line of the cell plate, the phragmoplast contour could also be distinguished. This fluorescence was not due to non-specific binding of PDL antibody to microtubules, since no mitotic spindle staining was observed in metaphase and early anaphase cells (Figure 6A).

PDL protein is located across the center of the phragmoplasts

It has long been suggested that the Golgi-derived vesicles are transported to the cell plate along the phragmoplast microtubules and/or microfilaments (Baskin and Cande, 1990). To study the possible relationship between PDL and microtubules, a double labeling experiment with both PDL protein and microtubule antibody was performed, and cells were then visualized with a confocal microscope. As shown in Figure 7, a metaphase spindle (cell #1) and phragmoplasts at different stages of cytokinesis (cell #2, 3, 4 and 5) could be clearly distinguished with microtubule labeling. PDL staining confirmed the result that PDL was associated with cell plate formation. The bright lines of fluorescence of PDL in Figure 7A corresponded exactly to the dark lines between the two sets of phragmoplast microtubules, which marked the position of cell plates in Figure 7B. No PDL staining was observed in metaphase cells (cell #1). The concentration of PDL protein seemed closely related to the concentration of the phragmoplast microtubules. Cells at the early stages of cytokinesis had highly concentrated phragmoplast microtubules, and the fluorescence of PDL protein was also brighter at these stages (compare cells #2 and #5). As the cell plate grew outwards, both the PDL protein and the microtubules decreased in the middle of the phragmoplasts (see cells #4 and #5). These data suggested that PDL was associated with the Golgi-derived vesicles that are transported to the cell equator region by phragmoplast microtubules. Whether PDL could interact directly with microtubules, as has been shown *in vitro* for dynamin and VPS1 (Obar *et al.*, 1990; Yeh *et al.*, 1991), remains unknown.

Even though the concentrations of both PDL and microtubules decreased in the middle of phragmoplasts as

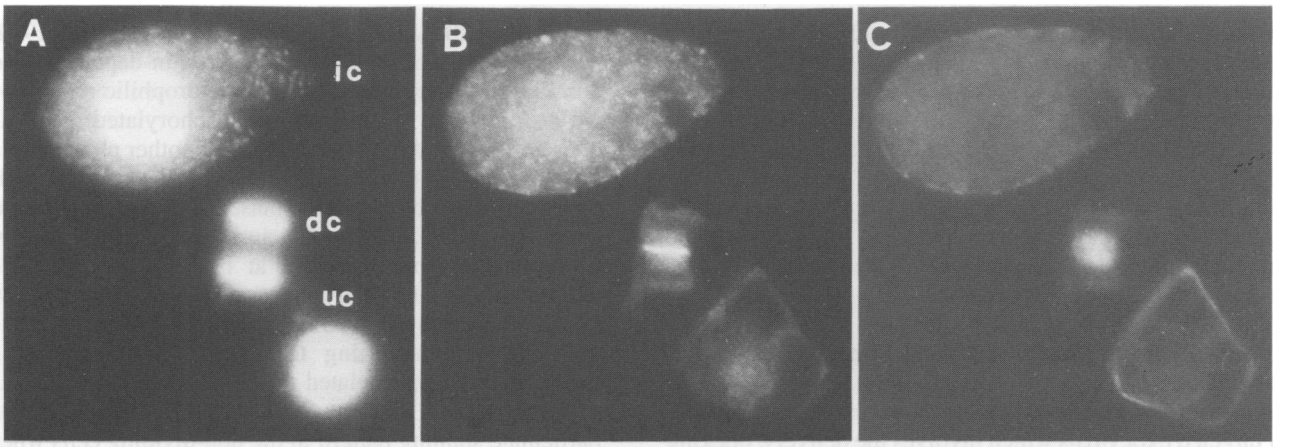

Fig. 8. Localization of PDL in soybean root nodule cells. ic, infected cell. dc, dividing cell. uc, uninfected cell. (**A**) DAPI staining showing nuclei and rhizobia. (**B**) Anti-PDL antibody staining showing the localization of PDL in nodule cells. Note the strong staining of the cell plate in the dividing nodule cells and the paticulate staining pattern in the infected cell. (**C**) Anti-tubulin antibody staining showing the distribution of microtubules.

the cell plate matured, the decrease of PDL was much slower than that of microtubules. A bright fluorescence line of PDL protein was still visible at the end of cytokinesis when the phragmoplast microtubules almost disappeared (cell #5), indicating that PDL protein participated in an event that was preceded by microtubule rearrangement and was not dependent on the organization of microtubules. These results thus demonstrated that PDL was associated with cell plate formation in phragmoplasts. Accordingly, we termed this protein 'phragmoplastin', a phragmoplast-associated protein marking the position of the cell plate in plants. Soybean PDL antibodies also cross-reacted with tobacco cells (data not shown), which suggests that this protein is highly conserved in plants.

PDL protein was also present in the non-dividing cells, as indicated by Western blot data, but it was present throughout the cells and a diffused particulate staining pattern could be observed. It seemed that both the increase in concentration of PDL protein and the accumulation of vesicles on the cell plate made the visualization of phragmoplastin possible during cytokinesis.

Localization of PDL in root nodules

Eleven-day-old soybean root nodules were used to study the location of PDL in infected and uninfected cells. At this stage, both infected cells and the dividing cells are easily visible in the nodule cell population. As shown in Figure 8, PDL was localized in the cell plate of the dividing cells in root nodules similar to that in root tips. The infected cells also showed enhanced fluorescence. In general, the fluorescence in the infected cells was much stronger than that in uninfected cells. Similarly to the non-dividing cells in root tips, the infected cells and non-dividing uninfected cells in nodules gave a particulate pattern of fluorescence. When compared with the DAPI staining pattern of the bacteria in the infected cells, it seemed that PDL was not associated with the peribacteroid membrane (PBM). The particulate localization pattern may be resolved at the electron microscopic level.

Discussion

Phragmoplastin is related to the dynamin protein family

Dynamin family proteins have diverse functions in animal and yeast cells (Shpetner and Vallee, 1992; Gout *et al.*, 1993; Herskovits *et al.*, 1993b; Staeheli *et al.*, 1993; Miki *et al.*, 1994; Seedorf *et al.*, 1994). Recently, it was observed that both Mx and dynamin can self-assemble into ring-like structures that have been shown to wrap around the endocytic vesicles (Hinshaw and Schmid, 1995; Takei *et al.*, 1995). It has been proposed that the ability to self-assemble into helices around a cylindrical structure might be a common link between the dynamin proteins (Kelly, 1995). Two possible self-association domains have been identified in Mx, including the leucine zipper motif in the C-terminal region and the self-assembly motif in the N-terminal region (Melen *et al.*, 1992; Nakayama *et al.*, 1993). The self-assembly motif in the N-terminal region is highly conserved among dynamin-related proteins.

We identified a plant dynamin-like protein which is involved in yet another different cellular process resembling exocytosis (see below). An *Arabidopsis* sequence homologous to dynamin was deposited recently in the Genbank database. In addition, PDL antibody can recognize a protein band from tobacco with similar molecular weight which is located on the cell plates of dividing cells (Gu and Verma, unpublished data). This evidence suggests the conservation of phragmoplastin in plants. There are 58% identical residues and up to 87% similarity in the first 300 amino acids between phragmoplastin and dynamin. The self-assembly motif is also highly conserved in phragmoplastin. It is conceivable that, like other members of this family, phragmoplastin can also self-assemble into polymers. The insolubility data seem to support this notion. Rat brain dynamin exists in detergent-soluble and detergent-insoluble forms (Liu *et al.*, 1994). We also found that phragmoplastin is present in multiple forms in plants. The detergent-insoluble fraction of phragmoplastin is highly insoluble at high concentrations of salt and remains

in the pellet even after extraction with 8 M urea. No transmembrane domains or sequences that modify proteins for membrane association were found in phragmoplastin. Similar results have been reported for Mx proteins (Melen *et al.*, 1992). It has been shown that the insolubility of Mx is due to aggregation and the formation of Mx polymers. The ability of phragmoplastin to form insoluble aggregates strongly suggests that this protein may be present as polymers, possibly associated with the transporting vesicles in plant cells.

Possible role of phragmoplastin in cell plate formation

The formation of the cell plate is, in essence, a process of targeted exocytosis which involves the delivery, docking and fusion of the transport vesicles. The vesicles are transported to the cell equator region by phragmoplast microtubules. The vesicle membranes fuse together to give rise to the new plasma membrane, while the cell wall polysaccharides carried by these vesicles later assemble to form the new cell wall. In addition to the normal process of exocytosis, the formation of the cell plate requires a new mechanism to confine the cell plate in a single plane to form a disc-like structure rather than an amorphous aggregate. Specific proteins are likely to be required to perform this function.

Membrane docking and fusion during cell plate development is a continuous process. It is noteworthy that the vesicles do not simply fuse to form large discs during early stages of cytokinesis, but rather give rise to the so-called 'branched bodies' (Jones and Payne, 1978; Hepler, 1982). It has been found that the branches of these 'stellate-shaped' bodies are confined to the plane of the cell plate. The 'branched bodies' then consolidate into flattened lamellae during the final stage of cell plate development, just before the fusion of the cell plate with the parental plasma membrane. We detected phragmoplastin at the very early stage of cell plate formation. The cell plate begins to fluoresce with the phragmoplastin antibodies soon after the formation of the phragmoplast. The presence of phragmoplastin on the cell plate continues until a very late stage, when the cell plate almost reaches the parental cell wall. Unlike the phragmoplast microtubules, there is less decrease in the fluorescence intensity in the middle of the cell plate as the phragmoplasts grow outwards, suggesting that PDL protein is not involved in the delivery of these vesicles. Based on the observations that other dynamin-like proteins can wrap around the elongated vesicles, it is possible that phragmoplastin participates in 'squeezing' the contents of the vesicles for cell plate formation. From the published electron micrographs (Hepler, 1982), we noticed that the branched bodies of the cell plate have a similar diameter and morphology to the elongated tubules formed by dynamin on the plasma membrane in the presence of GTP-γ-S (Takei *et al.*, 1995). Polymerization of phragmoplastin around the elongated tubules, as has been observed for dynamin (Takei *et al.*, 1995), may allow exocytic release of the contents of the vesicles for deposition on the cell plate. The exact process of exocytosis remains to be demonstrated.

The cell plate begins to form at late anaphase when chromosomes are separated. A calcium/calmodulin-dependent protein kinase II has been identified to be involved in the onset of anaphase (Morin *et al.*, 1994). Phragmoplastin has a calcium/calmodulin-dependent protein kinase II site at its C-terminal hydrophilic region, but we do not know whether it is phosphorylated. This site does not exist in dynamin, which has another phosphorylation site at the C-terminus and has been shown to be phosphorylated by protein kinase C in nerve terminals (Robinson *et al.*, 1993). Calcium and calmodulin have been reported to be present at high concentrations in phragmoplasts and cell plates (Wolniak *et al.*, 1980; Saunders and Hepler, 1981; Gunning and Wick, 1985). It will be very interesting to test if phragmoplastin is temporarily phosphorylated during cell plate formation.

We observed that the phragmoplastin gives a faint particulate staining pattern in the non-dividing cells where it may be simply associated with the vesicles normally fusing with plasma membrane for depositing cell wall material. This activity is much lower and dispersed, and follows the disappearance of the intense phragmoplastin staining soon after the completion of cytokinesis. The possible role of phragmoplastin in exocytosis of cell wall components from Golgi vesicles appears mechanically similar to endocytosis in the sense that it 'pinches or squeezes' the vesicles. However, a role similar to animal dynamin in endocytic recycling of the membrane vesicles after exocytosis cannot be ruled out completely at this stage, even though there is little evidence to suggest that endocytic recycling of membrane vesicles occurs during cell plate formation.

Proliferation of the PBMs in infected root nodule cells requires extensive membrane transport and fusion activity. The strong staining of the infected cells by PDL antibody suggests that PDL might be involved in PBM formation, but the localization pattern does not correlate with the PBM. Another unique feature of the nodule development is the formation and growth of infection threads, which requires targeted delivery and fusion of vesicles to the growing infection thread. The infection thread formation involves some processes similar to that of cell division (van Brussel *et al.*, 1992). Nod factor has been shown to be able to induce the 'pre-infection thread'/phragmosome formation in the outer cortex and cell division in the inner cortical cells at the same time. Both the formation of cell plate and the growth of the infection thread require transport and fusion of Golgi-derived vesicles. It would be of great interest to see if PDL is also involved in the growth of the infection thread in root nodules.

Materials and methods

Cloning of cDNA encoding dynamin-like protein from soybean

PDL cDNA clones were obtained using a PCR approach. One pair of oligonucleotides, 5′-CCI(AC)G(AC)GG(AT)(AT)(GC)TGGIAT(TC)G-TIAC-3′ and 5′-TTT(TG)GTIA(AT)(AG)ACICC(ATG)ATIGT-3′, corresponding to the conserved amino acid sequence PRGTGIVT in the dynamin signature sequence and TIGVLTK in the G4 region of the GTP binding domain, were synthesized and used as the primers. Soybean nodule poly(A) RNA was isolated from 15-day-old root nodules and reverse transcribed into cDNA using oligo(dT). PCR was performed as 45 cycles of 94°C for 40 s/55°C for 40 s/72°C for 1 min. The 500 bp fragment obtained was blunt-end ligated into the *Sma*I site of pUC19. A λ-ZapII soybean nodule cDNA library (Delauney and Verma, 1991) was then screened using this fragment as a probe. The positive clones were excised into plasmids *in vivo* following the standard procedure

(Stratagene). The two longest clones (pPDL5 and pPDL12) encoded by different genes were completely sequenced.

Expression of the PDL cDNA in E.coli, protein purification and antibody preparation

The *Bgl*II–*Kpn*I fragment of pPDL12 was cloned into the *Bam*HI–*Kpn*I site of bacterial expression vector pRSETC (Invitrogen) to give plasmid pEPDL-12. This vector contained a coding sequence for a polyhistidine metal binding domain to facilitate the purification of the expressed proteins. To make a construct which only contained the C-terminal half of the PDL protein, pEPDL-12 was cut with *Hin*cII and then re-ligated to give plasmid pEPDL-12ΔHc. The truncated protein contained only the last 353 amino acids; the N-terminal 257 amino acids, including the GTP binding domain, were removed. The construct was then transformed into *E.coli* Lys-s cells. The transformed cells were grown in LB medium and the proteins were induced by adding 0.5 mM IPTG.

PDL protein was purified by Ni affinity chromatography under non-denaturing conditions following the manufacturer's instructions (Invitrogen). The purified protein was then used for GTPase assay. Since most of the expressed protein was found in the inclusion body fraction, a denaturing method was used to purify PDL for antibody preparation. After Ni column chromatography under denaturing conditions, PDL protein was purified further by SDS–PAGE. The protein band was cut out from the acrylamide gel, ground in liquid nitrogen and used directly to inject rabbits. Antibody was affinity-purified from immunoblots for immunocytochemistry.

GTPase assay

GTPase assay was performed in 25 μl of reaction mixture containing 50 mM Tris–HCl (pH 8.0), 5 mM $MgCl_2$, 0.1 mM dithiothreitol, 130 μM or 13 μM cold GTP, 13 nM [α-^{32}P]GTP (1 μCi, 3000 Ci/mmol) and 0.1 μg of purified proteins. The reaction was carried out at 37°C for 60 min. Aliquots (0.5 μl) of the reaction products were applied to polyethyleneimine (PEI) cellulose plates, and GTP was separated from GDP by TLC in a solution containing 1.6 M LiCl and 1 M HAc (Nakayama *et al.*, 1991).

RNA isolation and Northern hybridization

Total RNA from 4-day-old root tips, 4-day-old root elongation zones and root nodules at different stages was isolated according to the method of Verwoerd *et al.* (1989). Northern bloting was performed at 68°C using a ^{32}P-labeled *Eco*RI–*Xho*I fragment of pPDL12 following the method of Mahmoudi and Lin (1989).

Subcellular fractionation and Western blot analysis

Fresh plant tissues were ground in liquid nitrogen with a pestle and mortar and then homogenized in ice-cold TB buffer (25 mM Tris–HCl pH 8.0, 5 mM EDTA, 1 mM 2-mercaptoethanol, 0.5 mM phenylmethylsulfonyl fluoride, 1 mM leupeptin) containing 17% (w/v) sucrose. The homogenate was passed through one layer of Miracloth and centrifuged at 10 000 *g* for 10 min. The pellet, which contains the nuclei, mitochondria and cell debris, was discarded and the supernatant (S10) was centrifuged at 100 000 *g* for 30 min to give a soluble fraction (S100) and a microsomal pellet (P100). To test the solubility of PDL in sodium carbonate, the pellet was resuspended directly in 0.1 M Na_2CO_3 (pH 11) at a protein concentration of 1 mg/ml. For other solubility experiments, crude microsomal membrane fraction was resuspended in the homogenization buffer at a concentration of 1 mg/ml and then 1/10 volume of 5 M NaI, 10% Triton X-100, 10% DOC or 10% SDS were added. The mixtures were placed on ice for 30 min, and centrifuged at 100 000 *g* for 30 min. Pellets were then resuspended in the same volume of homogenization buffer as the supernatant and subjected to SDS–PAGE.

Western bloting was performed using the ECL Western blot system (Amersham). Since the background reaction was very low, we routinely used the unpurified antiserum at a dilution of 1:500 for Western blots.

Immunofluorescence localization of phragmoplastin

Immunofluorescence microscopy was carried out by following the methods of Wick *et al.* (1981) with some modifications. Briefly, 4-day-old soybean root tips or 11-day-old nodules were fixed in 4% paraformaldehyde in PHEM (60 mM PIPES, 25 mM HEPES, 10 mM EGTA, 2 mM $MgCl_2$, pH 7.0) for 2 h at room temperature and then washed with buffer (10 mM MES, pH 5.7, 30 mM $CaCl_2$, 0.1% BSA, 5 mM 2-mercaptoethanol, 0.4 M mannitol) for 30 min. The plant tissues were then digested in a solution containing 2% cellulase (Calbiochem), 1% macerozyme R-10 (Ykult), 0.5% pectolyase Y23 (Karlan) in washing buffer for 15 min. After rinsing in PHEM buffer, the plant tissues were squashed between coverslips to release the individual cells. The cells were air dried for 10 min and then permeablized with 0.5% Triton X-100 in PHEM for 5 min. Immunofluorescence microscopy was carried out following the standard methods, using the affinity-purified anti-PDL IgG as the first antibody and the FITC-conjugated anti-rabbit goat IgG as a second antibody. Pre-immune serum was used as the first antibody in the control group. For double labeling experiments, mouse anti-tubulin IgG (Amersham) and TRITC-conjugated goat anti-mouse IgG (Sigma) were used to stain microtubules. DNA was stained with DAPI at a concentration of 10 μg/ml for 5 min at room temperature. Photographs were taken in phase contrast, and using appropriate filters for FITC and DAPI stainings. Double-labeled cells were visualized in a confocal microscope equipped with dual excitation/emission filter sets for both FITC and TRITC.

Accession numbers

PDL sequences reported in this paper have been submitted to the GenBank/EMBL data bank with the accession numbers U25547 for PDL12 and U36430 for PDL5.

Acknowledgements

We wish to thank Dr A.van der Bliek for providing *C.elegans* dynamin sequence data prior to publication and Drs Z.Yang and Y.Lin for help in immunolocalization. We also wish to thank Dr J.Herskovits for providing rat dynamin antibodies, Dr S.Emr for providing the yeast *vps1* mutant and Drs B.Oakley and A.Osterfeld for assistance in fluorescence microscopy. We also acknowledge the assistance of Mr D.Zdobinski with some parts of this study. The comments of Dr Z.Hong on this manuscript are appreciated. This work was supported by NSF grants MCB 8819399 and DCB 8904101.

References

Baskin,T.I. and Cande,W.Z. (1990) *Annu. Rev. Plant Physiol. Plant Mol. Biol.*, **41**, 277–315.

Bourne,H.R., Sander,D.A. and McCormick,F. (1991) *Nature*, **349**, 117–127.

Chen,M.S., Obar,R.A., Schroeder,C.C., Austin,T.W., Poodry,C.A., Wadsworth,S.C. and Vallee,R.A. (1991) *Nature*, **35**, 583–586.

Delauney,A. and Verma,D.P.V. (1991) In Gelvin,S.B., Schilperoort,R.A. and Verma,D.P.S. (eds), *Plant Molecular Biology Manual*. Kluwer Academic Publishers, pp. A14/1–12.

Fishkind,D.J. and Wang,Y. (1995) *Curr. Opin. Cell Biol.*, **7**, 23–31.

Fujiki,Y., Hubbard,A.L., Fowler,S. and Lazarow,P.B. (1982) *J. Cell Biol.*, **93**, 97–102.

Gout,I. *et al.* (1993) *Cell*, **75**, 25–36.

Gunning,B.E.S. and Wick,S.M. (1985) *J. Cell Sci. Suppl.*, **2**, 157–179.

Hepler,P.K. (1982) *Protoplasma*, **111**, 121–133.

Hepler,P.K. and Bonsigore,C.L. (1990) *Protoplasma*, **157**, 182–192.

Herskovits,J.S., Burgess,C.C., Obar,R.A. and Vallee,R.B. (1993a) *J. Cell Biol.*, **122**, 565–578.

Herskovits,J.S., Shpetner,H.S. and Burgess,C.C.(1993b) *Proc. Natl Acad. Sci. USA*, **90**, 11468–11472.

Hinshaw,J.E. and Schmid,S.L. (1995) *Nature*, **374**, 190–192.

Jones,M.G.K. and Payne,H.L. (1978) *Cytobios*, **20**, 79–91.

Kelly,R.B. (1995) *Nature*, **374**, 116–117.

Liu,J.P., Powell,K.A., Sudhof,T.C. and Robinson,P.J. (1994) *J. Biol. Chem.*, **269**, 21043–21050.

Mahmoudi,M. and Lin,V.K. (1989) *Biotechniques*, **7**, 331–333.

Melen,K., Ronn,T., Broni,B., Krug,R.M., von Bonsdorff,C. and Julkunen,I. (1992) *J. Biol. Chem.*, **267**, 25898–25907.

Miki,H., Miura,K., Matuoka,K., Nakata,T., Hirokava,N., Orita,S., Kaibuchi,K., Takai,Y. and Takenawa,T. (1994) *J. Biol. Chem.*, **269**, 5489–92.

Morin,N., Abrieu,A., Lorca,T., Martin,F. and Doree,M. (1994) *EMBO J.*, **13**, 4343–4352.

Nakayama,M., Nagata,K., Kato,A. and Ishihama,A. (1991) *J. Biol. Chem.*, **266**, 21404–21408.

Nakayama,M., Yazaki,K., Kusano,A., Nagata,K., Hanai,N. and Ishihama,A. (1993) *J. Biol. Chem.*, **268**, 15033–15038.

Obar,R.A., Collins,C.A., Hammarback,J.A., Shpetner,H.S. and Vallee,R.B. (1990) *Nature*, **347**, 256–261.

Poodry,C.A., Hall,L. and Suzuki,D.T. (1973) *Devel. Biol.*, **32**, 373–386.

Robinson,J.S., Klionsky,D.J., Banta,L.M. and Emr,S.D. (1988) *Mol. Cell. Biol.*, **8**, 4336–4948.
Robinson,P.J., Sontag,J., Liu,J., Fykse,E.M., Slaughter,C., McMahon, H. and Sudhof,T.C. (1993) *Nature*, **365**, 163–166.
Rothman,J.H., Raymond,T.G., O'Hara,P.J. and Stevens,T. (1990) *Cell*, **61**, 1063–1074.
Saunders,M.J, and Hepler,P.K. (1981) *Planta*, **152**, 272–281.
Seedorf,K., Kostka,G., Lammers,R., Bashkin,P., Daly,R., Burgess,W.H., van der Bliek,A.M., Schlessinger,J. and Ullrich,A. (1994) *J. Biol. Chem.*, **269**, 16009–16014.
Shpetner,H.S. and Vallee,R.B. (1989) *Cell*, **59**, 421–432.
Shpetner,H.S. and Vallee,R.B. (1992) *Nature*, **355**, 733–755.
Staeheli,P., Pitossi,F. and Pavlvic,J. (1993) *Trends Cell Biol.*, **3**, 268–272.
Takei,K., McPherson,P.S., Schmid,S. and Camilli,P.D. (1995) *Nature*, **374**, 186–190.
Vallee,R.B. and Okamoto,P.M. (1995) *Trends Cell Biol.*, **5**, 43–47.
van Brussel,A.A.N., Bakhuizen,R., Van Spronsen,P.C., Spaink,H.P., Tak,T., Lugtenberg,B.J.J. and Kijne,J.W. (1992) *Science*, **257**, 7072.
van der Bliek,A.M. and Meyerowitz,E.M. (1991) *Nature*, **351**, 411–414.
van der Bliek,A.M., Redelmerier,T.E., Damke,H., Tisdale,E.J., Meyerowitz,E.M. and Schmid,S.L. (1993) *J. Cell Biol.*, **122**, 553–563.
Vater,C.A., Raymond,C.K., Ekena,K., Howald-Stevenson,I. and Stevens,T. (1992) *J. Cell Biol.*, **119**, 773–786.
Verwoerd,T.C., Dekker,M.M. and Hoekema,A. (1989) *Nucleic Acids Res.*, **17**, 2362.
Wick,S.M., Seaguil,R.W., Osborn,M., Weber,K. and Gunning,B.E.S. (1981) *J. Cell Biol.*, **89**, 685–690.
Wilsbach,K. and Payne,G.S. (1993) *EMBO J.*, **12**, 3049–3059.
Wolniak,S.M., Hepler,P.K. and Jackson,W.T. (1980) *J. Cell Biol.*, **87**, 23–32.
Wolniak,S.M. and Larsen,P.M. (1995) *Plant Cell*, **7**, 431–445.
Yeh,E., Driscoll,R., Coltrera,M., Olins,A. and Bloom,K. (1991) *Nature*, **249**, 713–715.

Received on July 21, 1995; revised on October 30, 1995